HHS Public Access

Author manuscript

Neuropharmacology. Author manuscript; available in PMC 2019 October 01.

Published in final edited form as:

Neuropharmacology. 2018 October ; 141: 238–248. doi:10.1016/j.neuropharm.2018.09.003.

Disrupting interaction of PSD-95 with nNOS attenuates hemorrhage-induced thalamic pain

Weihua Cai[1,2,3], **Shaogen Wu**[1], **Zhiqiang Pan**[1], **Jifang Xiao**[1], **Fei Li**[4,5], **Jing Cao**[2,3], **Weidong Zang**[2,3,†], and **Yuan-Xiang Tao**[1,†]

[1]Department of Anesthesiology, New Jersey Medical School, Rutgers, The State University of New Jersey, Newark 07103, NJ, USA

[2]Department of Human Anatomy, School of Basic Medical Sciences, Zhengzhou University, Zhengzhou 450001, Henan, China

[3]Neuroscience Research Institute, College of Basic Medicine, Zhengzhou University, Zhengzhou 450001, Henan, China

[4]Department of Medicinal Chemistry, School of Pharmacy, Nanjing Medical University, Nanjing, Jiangsu 211166, China

[5]Collaborative Innovation Center for Cardiovascular Disease Translational Medicine, Nanjing Medical University, Nanjing, Jiangsu 211166, China.

Abstract

Hemorrhages occurring within the thalamus lead to a pain syndrome. Clinical treatment of thalamic pain is ineffective, at least in part, due to the elusive mechanisms that underlie the induction and maintenance of thalamic pain. The present study investigated the possible contribution of a protein-protein interaction between postsynaptic density protein 95 (PSD-95) and neuronal nitric oxide synthase (nNOS) to thalamic pain in mice. Thalamic hemorrhage was induced by microinjection of type IV collagenase into unilateral ventral posterior medial/lateral nuclei of the thalamus. Pain hypersensitivities, including mechanical allodynia, heat hyperalgesia , and cold allodynia, appeared at day 1 post-microinjection, reached a peak 5–7 days post-microinjection, and persisted for at least 28 days post-microinjection on the contralateral side. Systemic pre-treatment (but not post-treatment) of ZL006, a small molecule that disrupts PSD-95-nNOS interaction, alleviated these pain hypersensitivities. This effect is dose-dependent. Mechanistically, ZL006 blocked the hemorrhage-induced increase of binding of PSD-95 with nNOS and membrane translocation of nNOS in thalamic neurons. Our findings suggest that the

[†]Corresponding authors: Yuan-Xiang Tao, Department of Anesthesiology, New Jersey Medical School, Rutgers, The State University of New Jersey, 185 S. Orange Ave., MSB, E-661, Newark, NJ 07103. Tel: +1-973-972-9812; Fax: +1-973-972-1644. yuanxiang.tao@njms.rutgers.edu or Weidong Zang, Department of Human Anatomy, School of Basic Medical Sciences, Zhengzhou University, 100 Science Avenue, Zhengzhou, Henan, 450001, P. R. China. zwd@zzu.edu.cn.

Conflicts of interest

The authors have no conflicts of interest to disclose.

protein-protein interaction between PSD-95 and nNOS in the thalamus plays a significant role in the induction of thalamic pain. This interaction may be a promising therapeutic target in the clinical management of hemorrhage-induced thalamic pain.

Keywords

PSD-95; nNOS; protein-protein interaction; thalamic pain; hemorrhage

1. Introduction

As a leading cause of disability in industrialized countries, strokes produce huge health and economic burdens to a patient's family. Globally, there were approximately 6.5 million stroke-related deaths in 2013 (Benjamin et al., 2017). Stroke is often caused by brain ischemia and hemorrhage. Under both of these conditions, the affected brain areas display functional losses. Although epidemiologic studies reveal that hemorrhagic strokes only make up 8–18% of strokes, they exhibit higher rates in mortality than ischemic stroke (Feigin et al., 2003). Approximately 8–14% of stroke victims suffer from central post-stroke pain (Kumar and Soni, 2009), particularly when a hemorrhagic stroke occurs in thalamic regions. Clinical treatment of central post-stroke pain, including medications such as opioids, is often ineffective and/or has potential side effects (Gonzales, 1995; Nicholson, 2004). Understanding the cause of hemorrhagic-induced thalamic pain may provide a new avenue for the management of this disorder.

A numerous amount of animal experiments as well as clinical studies have shown that brain injury caused by stroke involves complex pathophysiological processes, including inflammatory damage (Kuan et al., 2015), abnormal microglia activation (Zhao et al., 2015), apoptosis and neurovascular damage (Wei et al., 2013), blood-brain barrier damage (Zeynalov et al., 2017), oxidative stress (Anderson et al., 2013) and the generation of free radical (Kikuchi et al., 2013). It is well documented that ischemia and hemorrhage immediately lead to sustained activation of excitatory N-methyl-D-aspartate (NMDA) receptors, and subsequently cause excessive activation of downstream effectors, including neuronal nitric oxide synthase (nNOS) (Khan et al., 2015). Overproduction of nitric oxide (NO) is thought to promote cell death and brain damage (Hara et al., 1996; Huang et al., 1994). The protein postsynaptic density protein-95 (PSD-95), also known as SAP-90 (synapse-associated protein 90), is one of a growing superfamily of PDZ-domain-containing proteins at central synapses. The PDZ domains of PSD-95 bind to NMDA receptor subunits NR2A and NR2B on its COOH-terminus tSXV motif, as well as to the PDZ domain of nNOS (Brenman et al., 1996; Christopherson et al., 1999; Kornau et al., 1995). Brain PSD-95 is required for excessive NMDA receptor activation-induced abnormal production of NO, therefore, neurotoxicity under stroke conditions (Aarts et al., 2002; Sattler et al., 1999). Disrupting the interaction between nNOS and PSD95 in the brain inhibited neurotoxic NO production and protected neurons from excitotoxicity and ischemic stroke (Zhou et al., 2010; Hu et al., 2013; Wu et al., 2014; Mo et al., 2016; Lin et al., 2018; Luo et al., 2014; Wang et al., 2017). PSD-95 is also required for NMDA receptor-mediated thermal hyperalgesia and nerve injury-induced neuropathic pain at the spinal cord level (Tao et al.,

2001; Tao et al., 2000). Perturbing the interaction between nNOS and PSD95 alleviated acute thermal hyperalgesia, formalin-induced nociceptive behaviors and inflammation-/nerve injury-induced pain hypersensitivity (Florio et al., 2009; Carey et al., 2017; Lee et al., 2015). However, whether or not PSD-95 and its interaction with nNOS participate in ischemia- or hemorrhage-induced thalamic pain is unknown. Like NMDA receptor antagonists, blocking PSD-95 expression may be impractical in a clinical setting, as both PSD-95 and NMDA receptors are widely expressed in the central nervous system and participate in many processes, including several forms of learning and memory (28;29). Directly targeting PSD-95 and NMDA receptors may produce adverse effects such as memory impairment, psychotomimetic effects, and ataxia (Chizh and Headley, 2005; Parsons, 2001). In contrast, targeting interaction of PSD-95 with nNOS may serve as a promising strategy in hemorrhage-induced thalamic pain, perhaps without major side effects since normal expression and function of NMDA receptors and PSD-95 are maintained (Zhou et al., 2010).

In the present study, we first characterized a mouse model of hemorrhage-induced thalamic pain by microinjection of type IV collagenase (Coll IV) into unilateral ventral posterior medial nuclei (VPM) and ventral posterior lateral nuclei (VPL) of the thalamus. We then examined whether intraperitoneal (i.p.) administration of ZL006, a small molecular inhibitor of the PSD-95-nNOS interaction to easily cross the blood-brain barrier (Florio et al., 2009; Zhou et al., 2010), affected hemorrhage-induced thalamic pain. Finally, we investigated whether the ZL006's effect was mediated by disrupting the PSD-95-nNOS interaction and blocking membrane translocation of nNOS in the thalamus.

2. Methods

2.1 Animal preparations

CD1 male mice (7–8 weeks) were obtained from Charles River Laboratories (Wilmington, MA). All mice were housed in an animal facility and kept in a standard 12-h light/dark cycle, with free access to standard laboratory water and food pellets. Animal experiments were conducted with the approval of the Animal Care and Use Committee at New Jersey Medical School (Rutgers IACUC Approval #17003) and all the experiments were performed in accordance with the ethical guidelines of the US National Institutes of Health and the International Association for the Study of Pain. All efforts were made to minimize animal suffering and reduce the number of animals used. To minimize intra- and inter-individual variability of behavioral outcome measures, animals were trained for 1–2 days before behavioral testing was performed. The experimenters were blinded to treatment condition during behavioral testing.

2.2 Hemorrhage-induced thalamic pain model

The thalamic hemorrhage was conducted based on the previous work done on rats, with some modifications (Kuan et al., 2015). Briefly, mice were anesthetized using vaporized isoflurane (5% induction, 2% maintenance) and placed in a stereotaxic frame. Under stereotaxic guidance, the animals were microinjected with Coll IV (Sigma-Aldrich Co., St. Louis, MO; 0.01 U/10 nl, dissolved in saline) into the right VPM and VPL of the thalamus

(anterior–posterior to bregma −0.82~− 2.30 mm: lateral to the midline 1.30~1.95 mm posterior, deep to the surface of the skull 3.01~4.25 mm). In the sham groups, 10 nl of sterile saline was injected. The glass micropipette was maintained in the place for 10 min after administration to allow Coll IV dispersed completely. The glass micropipette was slowly pulled out. After microinjection, the surgical field was irrigated with sterile saline and iodophor and closed with wound clips.

2.3 Behavioral tests

Mechanical test through the measurement of paw withdrawal frequencies in response to mechanical stimuli was first carried out as described previously (Li et al., 2017). Briefly, mice were placed individually in a plexiglas chamber on an elevated mesh screen and allowed to habituate for 30 min. Two calibrated von Frey filaments (0.07 and 0.4 g, Stoelting Co.) were applied to the hind paw for approximately 1 s. Each filament was applied to the hid paw 10 times with 5 min interval for each side hind paw. The experiments were done on both sides first with the 0.07 g filament and then with the 0.4 g filament. A quick withdrawal of the paw was regarded as a positive response. Paw withdrawal responses to each of these 10 times stimuli were counted as a percent response frequency: [(number of paw withdrawals/10 trials) × 100% = response frequencies].

Heat test through the measurement of paw withdrawal latencies to noxious heat was then performed with a Model 336 Analgesia Meter (IITC Inc. Life Science Instruments. Woodland Hills, CA) as described (Li et al., 2015; Li et al., 2017; Xu et al., 2014; Zhao et al., 2013). Briefly, mice were placed in a Plexiglas chamber on a glass plate. A beam of light was emitted from the light box and applied on the middle of the plantar surface of each hind paw. A quick lift of the hind paw was regarded as a signal to turn off the light. The length of lighting beam time was defined as the paw withdrawal latency. For each side, five trials with 5-min interval time were carried out. A cutoff time of 20 s was used to avoid tissue damage.

Finally, cold test through the measurement of paw withdrawal latencies to noxious cold (0 °C) was carried out using a cold aluminum plate as described (Li et al., 2015; Li et al., 2017; Xu et al., 2014; Zhao et al., 2013). Briefly, each mouse was placed in a Plexiglas chamber on the plate with continuous temperature monitoring by a thermometer. The length of time between the placement and the sign of mouse jumping was defined as the paw jumping latency. Each trial was repeated three times at 10-min intervals. A cutoff time of 20 s was used to avoid tissue damage.

Locomotor functional tests (Li et al., 2017), including placing, grasping, and righting reflexes, were carried out after the pain behavioral tests described above were completed. For the placing reflex, the hind limbs were placed slightly lower than the forelimbs and the dorsal surfaces of the hind paws were brought into contact with the edge of a table. Then, whether the hind paws were placed on the table surface reflexively was recorded. For the grasping reflex, animals were placed on a wire grid, and then whether the hind paws grasped the wire on was recorded. For the righting reflex, animals were placed on its back on a flat surface, and it was recorded whether mouse could immediately assume the normal upright position. Each trial was repeated five times with 5-min interval and the score for each test was recorded by counting times of each normal reflex.

2.4 Histological localization of injection sites

Animals were deeply anesthetized with isoflurane and transcardially perfused with 50–100 ml of 4% paraformaldehyde in 0.1M phosphate buffered saline (PBS, pH 7.4). The brain was removed, post-fixed overnight at 4 °C, and cryoprot ected in 30% sucrose in 0.1 M PBS for two days. The brain was sectioned at the thickness of 30 μm and subjected to cresyl violet (Nissl) staining as described previously (Liaw et al., 2005) with slight modification. Briefly, after being dehydrated, the sections were stained in 0.1% cresyl violet solution at 37°C for 30 min. The sections were then rinsed in distilled water for 2 times and differentiated in 95% ethyl alcohol with 2 drops glacial acetic acid for 15 min. The localization and size of the damage were identified under a light microscope. The lesion areas were analyzed by Image J.

2.5 Subcellular fractionation

Subcellular fractionation was carried out as described previously (Park et al., 2009; Tao et al., 2003). In brief, the tissues from the injected thalamus were homogenized in homogenization buffer containing 250 mM sucrose, 10 mM Tris-HCl (pH 7.4), 1 mM EDTA, and 1 mM PMSF, 1 mM benzamidine. After the homogenate was centrifuged at 1,000 × g for 15 min at 4°C, the supernatant (total soluble fraction) was collected and then centrifuged at 20,000 × g for 20 min at 4°C. The pellet (crude plasma membrane fraction) was collected.

2.6 CO-immunoprecipitation (Co-IP) assay

Co-immunoprecipitation was carried out according to the previous protocols (Park et al., 2009; Tao et al., 2003; Zhou et al., 2010). Briefly, crude plasma membrane fraction was dissolved in chilled lysis buffer A, containing 50 mM Tris-HCl [pH 7.4], 150 mM NaCl, 1 mM EDTA-Na, 1% NP-40, 0.02% sodium azide, 0.1% SDS, 0.5% sodium deoxycholate, 1% PMSF, and 1% protease inhibitor cocktails. The sample (400 μg) was subjected to immunoprecipitation with 1 μg of rabbit antibodies against PSD-95 (catalog number 2507S, Cell Signaling), or with 1 μg of normal rabbit serum for 3 h at 4 °C. Twenty μl of magnetic beads conjugated with protein A (cat. no. 16–661, Millipore Sigma-Aldrich) were then added into each sample before rotating shaker at 4°C for overnight. On the next day, the m ixture of magnetic beads and bound immunocomplexes was washed with the buffer containing 0.05M HEPES, 0.15M NaCl, and 0.15M Triton-100 (pH 7.4). The bound immunocomplexes were eluted by heating at 99 °C in 1X loading buffer and analyzed through Western blotting assay as described below.

2.7 Western blotting assay

Western blotting assay was carried out according to our previously published protocol (Li et al., 2017; Zhao et al., 2017). Briefly, the samples were heated at 99 °C for 5 min and loaded onto a 4–20% precast polyacrylamide gel (cat. no. 3450032, Bio-Rad Laboratories). The proteins were then electrophoretically transferred onto a polyvinylidene difluoride membrane (cat. no. #1620175, 0.2 μm, Bio-Rad Laboratories). The membranes were blocked with 3% nonfat milk in Tris-buffered saline containing 0.1% Tween-20 for 2 h and then incubated overnight with the primary antibodies, including rabbit anti-nNOS (1:400,

catalog number 610308, BD Transduction), mouse anti-PSD-95 (1:500, catalog number sc-32290, Santa Cruz Biotechnology), and rabbit anti-GAPDH (1:2,000, catalog number sc-25778, Santa Cruz Biotechnology), respectively. The proteins were detected by goat peroxidase–conjugated anti-mouse (1:3,000, catalog number 115-035-003, Jackson ImmunoResearch) or anti-rabbit secondary antibody (1:3000, catalog number 111–035003, Jackson ImmunoResearch) and visualized by western peroxide reagent and luminol/ enhancer reagent (catalog number 170–5060, Clarity Western ECL Substrate, Bio-Rad) and exposure using ChemiDoc XRS System with Image Lab software (Bio-Rad). The intensity of blots was quantified with densitometry using Image Lab software (Bio-Rad).

2.8 Single-cell real-time reverse transcription-polymerase chain reaction (RT-PCR)

After the mice were euthanized with isoflurane, the thalamus was harvested in cold neurobasal medium (Gibco/ThermoFisher Scientific) containing 10% fetal bovine serum (JR Scientific, Woodland, CA), 100 units/ml Penicillin, and 100 mg/ml Streptomycin (Quality Biological, Gaithersburg, MD). The thalamus was then treated with enzyme solution containing 0.25% trypsin and 0.05% DNase I in Hanks' balanced salt solution (HBSS) without $Ca2^{+}$ and $Mg2^{+}$ (Gibco/ThermoFisher Scientific). After trituration and centrifugation, the dissociated neurons were suspended in the mixed neurobasal medium and then plated on cover glasses coated with 50 mg/ml poly-D-lysine (Sigma) in a six-well plate. Three hours after the neurons were incubated in 95% O_2 and 5% CO_2 at 37 °C, under an inverted microscope fit with a micromanipulator and microinjector, a single living thalamic neuron was collected in a PCR tube with 10 μl of cell lysis buffer (Signosis, Sunnyvale, CA). After centrifugation, the supernatants were harvested and divided into two PCR tubes, respectively, for *Nos1* (encoding nNOS protein) and *Dlg4* (encoding PSD-95 protein) mRNAs. The *Nos1* primer sequences were 5′-CACGAGGACATCTTTGGGGT -3′ (forward) and 5′- AGGAGCTGAAAACCTCATCTGT -3′ (reverse). The *Dlg4* primer sequences were 5′- AGATCACATTGGAAAGGGGTAA -3′ (forward) and 5′- ACCAGGAATGATCTTGGTGAT -3′ (reverse). The remaining real-time RT-PCR procedure was carried out based on the manufacturer's instructions with the single-cell real-time RT-PCR as described previously (Zhao et al., 2017).

2.9 Statistical analysis

Animals were distributed into various treatment groups randomly. All results are given as means ± S.E.M. The data were statistically analyzed with one-way ANOVA. Once ANOVA showed a significant difference, pairwise comparisons between means were analyzed by the post hoc Tukey method (SigmaPlot 12.5, San Jose, CA). Significance was set at $P < 0.05$.

3. Results

3.1 Hemorrhagic area and general behaviors

The hemorrhage area was estimated using serial cross-coronal brain sections 5–7 days after microinjection of Coll IV into the thalamus. These time points were chosen because pain behavioral responses reached a peak on days 5–7 after microinjection (see below). The hemorrhage was localized predominantly around the VPL and VPM of the thalamus, without extending into the internal capsule (Fig. 1A and 1B). The lesion was seen

approximately anterior–posterior to bregma from −1.06 mm to −2.30 mm (Fig 1A). The mean lesion size was 0.39 ± 0.07 mm^2 at day 5 after microinjection (n = 6). The number of integral cells in the ipsilateral VPL and VPM was visibly decreased compared to that in the contralateral ones (Fig. 1B). No bleeding was observed in other brain regions following microinjection of Coll IV at the dose and volume used (Fig. 1A and 1B). As expected, microinjection of saline into thalamus did not show significant bleeding and displayed normal thalamic structure (data not shown).

Following microinjection, all mice exhibited normal posture, gait, feeding, and drinking behaviors, without any signs of motor dysfunction during the observational period. Foot droop and autotomy were not seen in any injected mice. Their toes were spread apart when walking and standing. As shown in Supplementary Table 1, the Coll IV-injected mice showed normal placing, grasping and righting reflexes 14 days after microinjection.

3.2 Hemorrhage-induced thalamic pain

The hemorrhagic mice displayed robust and long-lasting mechanical allodynia, heat hyperalgesia, and cold allodynia on the contralateral side. Significant increases in paw withdrawal frequencies in response to 0.07 g and 0.4 g von Frey filaments (Fig. 2A and 2B) and marked reduction in paw withdrawal latencies to heat (Fig. 2C) and cold (Fig. 2D) stimuli were seen on the contralateral side after Coll IV microinjection. These pain hypersensitivities occurred 1 day after microinjection, reached a peak around 5–7 days after microinjection, and persisted for at least 28 days after microinjection (Fig. 2A-2D). As expected, saline microinjection did not significantly alter basal paw withdrawal frequencies and latencies on the contralateral side (Fig. 2A-2D). Neither Coll IV nor saline microinjection changed basal paw withdrawal frequencies and latencies on the ipsilateral side (Supplementary Fig. 1A-1C).

Given that previous studies revealed a benefit of gabapentin administration in post-stroke pain in clinic (Attal et al., 1998), we examined whether gabapentin had the effect on thalamic pain in our mouse model. Gabapentin, at 20 mg/kg, was injected intraperitoneally, respectively, on day 3 and day 14 after Coll IV or saline microinjection. Behavioral tests were carried out one day before Coll IV microinjection and before and 30 min after gabapentin injection on both day 3 and day 14 after Coll IV microinjection. Systemic administration of gabapentin significantly blocked the increases in paw withdrawal frequencies in responses to 0.07 g and 0.4 g von Frey filaments (Fig. 3A-3B and Supplementary Fig. 2A-2B) and rescued the decreases in paw withdrawal latencies to heat (Fig. 3C and Supplementary Fig. 2C) and cold (Fig. 3D and Supplementary 2D) stimuli on the contralateral side, respectively, on days 3 (Fig. 3A-3D) and 14 (Supplementary Fig. 2A-2D) after Coll IV microinjection. Gabapentin at the dosage used did not affect basal paw withdrawal frequencies and latencies on either day 3 or day 14 after saline microinjection (Fig. 3A-3D and Supplementary Fig. 2A-2D).

3.3 Pre-treatment of ZL006 attenuates hemorrhage-induced thalamic pain

We further examined whether systemic pre-administration of ZL006 affected hemorrhage-induced thalamic pain. Three doses (0.5, 3, and 10 mg/kg; dissolved in 5% $NaHCO_3$ plus

2% Tween-80) of ZL006 as well as vehicle (5% $NaHCO_3$ plus 2% Tween-80) were intraperitoneally administrated 30 min before Coll IV or saline microinjection (Fig. 4A). As expected, mechanical allodynia, thermal hyperalgesia, and cold allodynia developed 1, 3, and 5 days post-Coll IV microinjection on the contralateral side of the vehicle plus Coll IV-treated group compared to the vehicle plus saline-treated group (Fig. 4B-4E). I.p. pre-administration of ZL006 at 10 mg/kg significantly attenuated the increases in paw withdrawal frequencies in response to 0.07 g and 0.4 g von Frey filaments (Fig. 4B and 4C) and the decreases in paw withdrawal latencies to heat (Fig. 4D) and cold (Fig. 4E) stimuli on days 1, 3, and 5 post-Coll IV microinjection on the contralateral side of the ZL006 plus Coll IV-treated group. These effects were dose-dependent (Fig. 5A-5D). ZL006 at these doses used did not alter basal paw withdrawal frequencies and latencies on the ipsilateral side of the ZL006 plus Coll IV-treated group (Supplementary Fig. 3A-3C and Fig. 4A-4C) and on both contralateral (Fig. 4B-4E) and ipsilateral (Supplementary Fig. 3A-3C) sides of the ZL006 plus saline-treated group during the observation period. After behavioral tests, we collected brain tissues and performed the Nissl staining to examine whether the pre-treatment of ZL006 affected the Coll IV-induced thalamic lesion. As expected, numerous Nissl-stained cells were seen in the ipsilateral VPL and VPM of the saline plus vehicle- or ZL006-treated groups, whereas few Nissl-stained cells were detected in the ipsilateral VPL and VPM of the Coll IV plus vehicle-treated group (Fig. 6A and 6B). Compared with the Coll IV plus vehicle-treated group, the number of Nissl-stained cells was significantly increased in the ipsilateral VPL and VPM of the Coll IV plus ZL006-treated group, although it was still markedly lower than that in the saline plus vehicle- or ZL006-treated group (Fig. 6A and 6B). Interestingly, there were no visible differences in the areas of tissue damages between the Coll IV plus vehicle-treated and Coll IV plus ZL006-treated groups (Fig. 6A).

3.4 Post-treatment of ZL006 does not affect hemorrhage-induced thalamic pain.

We next asked whether systemic post-administration of ZL006 would alleviate hemorrhage-induced thalamic pain. After mice received i.p. injection with the highest dose of ZL006 (10 mg/kg) as well as vehicle 30 min after Coll IV or saline microinjection, behavior tests were carried out 1, 3, and 5 days after microinjection (Fig. 7A). Mechanical allodynia, heat hyperalgesia, and cold allodynia were seen in the contralateral side of both Coll IV plus vehicle or ZL006 groups at observed time points (Fig. 7B-7E). There were no marked differences in the Coll IV-induced increases in paw withdrawal frequencies in responses to 0.07 g and 0.4 g stimuli and in the Coll IV-induced decreases in paw withdrawal latencies in responses to heat and cold stimuli between the ZL-006 plus Coll IV-treated group and the vehicle plus Coll IV-treated group at the corresponding time points (Fig. 7B-7E). Consistent with the observation above, neither ZL006 nor vehicle altered basal paw withdrawal frequencies and latencies on the contralateral side after saline microinjection (Fig. 7B-7E) and on the ipsilateral side of all treated groups (Supplementary Fig. 5A-5C).

3.5 Pre-treatment of ZL006 disrupts the PSD-95-nNOS interaction in thalamic neurons

Finally, we confirmed whether ZL006 produced antinociceptive effect on hemorrhage-induced thalamic pain through disrupting PSD-95/nNOS protein-protein interaction in thalamic neurons. In the crude plasma membrane fraction from the thalamus, the level of nNOS and the binding density between PSD-95 and nNOS in the Coll IV plus vehicle-

treated group were significantly increased by 1.73-fold and 2.03-fold, respectively, compared to those in the saline plus vehicle-treated group (Fig. 8A). These increases were absent in the ZL006 plus Coll IV-treated group (Fig. 8A). Basal level of PSD-95 in the crude plasma membrane (Fig. 8A) and total amount of nNOS in whole membrane and cytoplasmic lysis (Fig. 8B) from the microinjected thalamus of the Coll IV plus vehicle- or ZL006-treated group were not changed compared to the saline plus vehicle-treated group. Single-cell RT-PCR analysis revealed that co-expression of *Nos1* mRNA with *Dlg4* mRNA in individual thalamic neurons (Fig. 8C).

4. Discussion

Thalamic hemorrhage caused by microinjection of Coll IV into the thalamus leads to long-term pain hypersensitivities including mechanical allodynia, thermal hyperalgesia, and cold allodynia in a mouse model, which mimics thalamic pain caused by hemorrhagic stroke in the clinic. Understanding the mechanisms that underlie hemorrhage-induced thalamic pain may allow for the development of a new therapeutic strategy for prevention and/or treatment of this disorder. Despite intensive research into hemorrhage-induced central post-stroke pain (including thalamic pain) in the past decades, how exactly central post-stroke pain develops after the stroke is still incomplete. The present study reported that the protein-protein interaction between PSD-95 and nNOS in thalamic neurons was required for the development of hemorrhage-induced thalamic pain. Thus, the PSD-95-nNOS interaction may be a potential target for therapeutic prevention of central post-stroke pain.

Although there is an increasing number of stroke survivors who experience central post-stroke pain (Akyuz and Kuru, 2016; Kumar et al., 2016; Vartiainen et al., 2016), the animal models used for studying central post-stroke pain (including thalamic pain) have not been well characterized. The animal models used for studying brain ischemia (e.g., middle cerebral artery occlusion) and hemorrhage (e.g., intracerebral hemorrhage) often cause changes in motor function, which significantly affects the evoked behavioral assessments (Akyuz and Kuru, 2016; Vartiainen et al., 2016). Blasi F et al. injected endothelin 1 (a potent vasoconstrictor) to induce a focal ischemic thalamic infarct, but this injection caused transient ischemia and late-onset (28 days later) minor thermal hyperalgesia (Akyuz and Kuru, 2016; Blasi et al., 2015; Vartiainen et al., 2016). It appears that pain behavioral responses in this model do not completely mimic central post-stroke pain in ischemic patients. The injection of Coll IV into the VPL of a mouse thalamus or the lateral nucleus and basal complex/posterior nucleus of a rat thalamus produced a long-term hemorrhage-induced central post-stroke pain (Hanada et al., 2014; Kuan et al., 2015; Yang et al., 2014). However, these injections also produced, to some extent, changes in motor function and/or bilateral pain behavioral alternations (Hanada et al., 2014; Kuan et al., 2015; Yang et al., 2014). The present study injected a smaller volume and a lower concentration of Coll IV into unilateral VPM and VPL of a mouse thalamus and revealed an early-onset and long-term pain hypersensitivities on the contralateral side without any signs of motor dysfunction. These pain hypersensitivities could be alleviated by systemic administration of gabapentin, a phenomenon that is consistent with the benefit of gabapentin in central post-stroke pain in a clinic (Attal et al., 1998). The distinct observations between the present study and previous works (Hanada et al., 2014; Kuan et al., 2015; Yang et al., 2014) may be attributed to the

differences in the volume and concentration of the injected Coll IV and the injected sites in the thalamus. Our model may be ideal to assess evoked pain hypersensitivities following thalamic hemorrhage.

Several mechanisms that participate in the development of central post-stroke pain have been proposed. Increased synaptic glutamate release and subsequently excessive activation of excitatory postsynaptic glutamate receptors (such as NMDA receptors) and extreme Ca^{++} influx into neuronal cells through these receptors in thalamus exacerbated the infarction and were involved in the stroke-related pain and allodynia (Takami et al., 2011). In another animal study, high doses of ketamine, an NMDA receptor antagonist, alleviated thalamic hemorrhage-induced mechanical allodynia (Castel et al., 2013). PSD-95 binds to both nNOS and NMDA receptor subunits NR2A and NR2B and is required for excessive NMDA receptor activation-triggered abnormal NO production and subsequent neurotoxicity/brain lesion through excess Ca^{++} influx (Aarts et al., 2002; Brenman et al., 1996; Christopherson et al., 1999; Kornau et al., 1995; Sattler et al., 1999; Zhou et al., 2010; Hu et al., 2013; Lin et al., 2018; Luo et al., 2014; Mo et al., 2016; Wu et al., 2014). The present study demonstrated that systemic pre-administration of ZL006 disrupted the Coll IV-induced increase in the PSD-95-nNOS protein-protein interaction and nNOS membrane translocation in thalamic neurons and prevented Coll IV-induced thalamic lesion, which is consistent with the previous reports that revealed that perturbing PSD-95-nNOS interaction with small molecules (such as ZL006) protected brain neurons from excitotoxicity and ischemic stroke (Hu et al., 2013; Lin et al., 2018; Mo et al., 2016; Wu et al., 2014; Zhou et al., 2010). More importantly, systemic pre-administration of ZL006 attenuated Coll IV-induced mechanical allodynia, heat hyperalgesia, and cold allodynia, suggesting that PSD-95-nNOS protein-protein interaction in thalamic neurons also participates in hemorrhage-induced thalamic pain. This conclusion is strongly supported by previous observations that disrupting the PSD-95-nNOS protein-protein interactions in the spinal cord suppressed the formalin-induced second pain behaviors, complete Freund's adjuvant-induced inflammatory pain, and paclitaxel- or chronic constriction injury-induced neuropathic pain (Carey et al., 2017; Florio et al., 2009; Lee et al., 2015). Our findings suggest that PSD-95-nNOS interaction in thalamic neurons plays a key role in the development of hemorrhage-induced thalamic pain.

Unexpectedly, post-administration of ZL006 did not affect thalamic hemorrhage-induced pain hypersensitivities. This suggests that other NMDA receptor/PSD-95/nNOS signaling pathway-independent mechanisms play a critical role in hemorrhage-induced thalamic pain once this pathway is activated. Consistent with this conclusion, prolonged microglia activation helped to maintain central post-stroke pain since microglial inhibition ameliorated stroke-induced pain hypersensitivities (Hanada et al., 2014). Neuroinflammation caused by chemokines and cytokines was involved in stroke-induced hyperalgesia (Tamiya et al., 2013). Moreover, thalamic P_2X_7 receptor directly participated in pain transmission and hypersensitivity under central post-stroke pain conditions, as blocking this receptor during the acute stage of hemorrhage rescued abnormal pain behaviors and neuronal activity in thalamocingulate pathway by reducing reactive microglial/macrophage aggregation and associated inflammatory cytokines (Kuan et al., 2015). In addition, P_2X_7 receptor expression was increased in reactive microglia/macrophages of thalamus 5 weeks post-hemorrhage (Kuan et al., 2015). Therefore, these NMDA receptor/PSD-95/nNOS independent signals in

thalamic neurons likely participate mainly in the maintenance of hemorrhage-induced thalamic pain.

In summary, this study has, for the first time, provided evidence that disrupting the thalamic hemorrhage-induced increase in PSD-95-nNOS protein-protein-interaction through systemic pre-administration of ZL006 was able to alleviate the thalamic hemorrhage-induced pain hypersensitivities without altering basal or acute nociceptive responses and locomotor functions. Given that ZL006 was proven to easily cross the blood-brain barrier and did not alter NMDA receptor functions (Florio et al., 2009; Lee et al., 2015; Zhou et al., 2010), this drug may serve as a potential therapy for hemorrhage-induced thalamic pain, perhaps without severe side effects.

Supplementary Material

Refer to Web version on PubMed Central for supplementary material.

Acknowledgements

This work was supported by the National Institutes of Health (R01NS094664, R01NS094224, and R01DA033390).

Reference List

1. Benjamin EJ, Blaha MJ, Chiuve SE, Cushman M, Das SR, Deo R, de Ferranti SD, Floyd J, Fornage M, Gillespie C, Isasi CR, Jimenez MC, Jordan LC, Judd SE, Lackland D, Lichtman JH, Lisabeth L, Liu S, Longenecker CT, Mackey RH, Matsushita K, Mozaffarian D, Mussolino ME, Nasir K, Neumar RW, Palaniappan L, Pandey DK, Thiagarajan RR, Reeves MJ, Ritchey M, Rodriguez CJ, Roth GA, Rosamond WD, Sasson C, Towfighi A, Tsao CW, Turner MB, Virani SS, Voeks JH, Willey JZ, Wilkins JT, Wu JH, Alger HM, Wong SS, Muntner P (Heart Disease and Stroke Statistics-2017 Update: A Report From the American Heart Association. Circulation 135:e146–e603.2017). CIR.0000000000000485 [pii];10.1161/CIR.0000000000000485 [doi] [PubMed: 28122885]
2. Feigin VL, Lawes CM, Bennett DA, Anderson CS (Stroke epidemiology: a review of population-based studies of incidence, prevalence, and case-fatality in the late 20th century. Lancet Neurol 2:43–53.2003). S1474442203002667 [pii] [PubMed: 12849300]
3. Kumar G, Soni CR (Central post-stroke pain: current evidence. J Neurol Sci 284:10–17.2009). S0022-510X(09)00578-4 [pii];10.1016/j.jns.2009.04.030 [doi] [PubMed: 19419737]
4. Gonzales GR (Central pain: diagnosis and treatment strategies. Neurology 45:S11–S16.1995).
5. Nicholson BD (Evaluation and treatment of central pain syndromes. Neurology 62:S30–S36.2004).
6. Kuan YH, Shih HC, Tang SC, Jeng JS, Shyu BC (Targeting P(2)X(7) receptor for the treatment of central post-stroke pain in a rodent model. Neurobiol Dis 78:134–145.2015). S0969-9961(15)00096-0 [pii];10.1016/j.nbd.2015.02.028 [doi] [PubMed: 25836422]
7. Zhao X, Sun G, Ting SM, Song S, Zhang J, Edwards NJ, Aronowski J (Cleaning up after ICH: the role of Nrf2 in modulating microglia function and hematoma clearance. J Neurochem 133:144–152.2015). 10.1111/jnc.12974 [doi] [PubMed: 25328080]
8. Wei S, Sun J, Li J, Wang L, Hall CL, Dix TA, Mohamad O, Wei L, Yu SP (Acute and delayed protective effects of pharmacologically induced hypothermia in an intracerebral hemorrhage stroke model of mice. Neuroscience 252:489–500.2013). S0306-4522(13)00646-5 [pii];10.1016/j.neuroscience.2013.07.052 [doi] [PubMed: 23912033]
9. Zeynalov E, Jones SM, Elliott JP (Therapeutic time window for conivaptan treatment against stroke-evoked brain edema and blood-brain barrier disruption in mice. PLoS One 12:e01839852017). 10.1371/journal.pone.0183985 [doi];PONE-D-17-12132 [pii] [PubMed: 28854286]

10. Anderson CD, Biffi A, Nalls MA, Devan WJ, Schwab K, Ayres AM, Valant V, Ross OA, Rost NS, Saxena R, Viswanathan A, Worrall BB, Brott TG, Goldstein JN, Brown D, Broderick JP, Norrving B, Greenberg SM, Silliman SL, Hansen BM, Tirschwell DL, Lindgren A, Slowik A, Schmidt R, Selim M, Roquer J, Montaner J, Singleton AB, Kidwell CS, Woo D, Furie KL, Meschia JF, Rosand J (Common variants within oxidative phosphorylation genes influence risk of ischemic stroke and intracerebral hemorrhage. Stroke 44:612–619.2013). STROKEAHA.112.672089 [pii]; 10.1161/STROKEAHA.112.672089 [doi] [PubMed: 23362085]

11. Kikuchi K, Miura N, Kawahara KI, Murai Y, Morioka M, Lapchak PA, Tanaka E (Edaravone (Radicut), a free radical scavenger, is a potentially useful addition to thrombolytic therapy in patients with acute ischemic stroke. Biomed Rep 1:7–12.2013). 10.3892/br.2012.7 [doi];br-01-01-0007 [pii] [PubMed: 24648884]

12. Khan M, Dhammu TS, Matsuda F, Singh AK, Singh I (Blocking a vicious cycle nNOS/peroxynitrite/AMPK by S-nitrosoglutathione: implication for stroke therapy. BMC Neurosci 16:422015). 10.1186/s12868-015-0179-x [doi];10.1186/s12868-015-0179-x [pii] [PubMed: 26174015]

13. Hara H, Huang PL, Panahian N, Fishman MC, Moskowitz MA (Reduced brain edema and infarction volume in mice lacking the neuronal isoform of nitric oxide synthase after transient MCA occlusion. J Cereb Blood Flow Metab 16:605–611.1996). 10.1097/00004647-199607000-00010 [doi] [PubMed: 8964799]

14. Huang Z, Huang PL, Panahian N, Dalkara T, Fishman MC, Moskowitz MA (Effects of cerebral ischemia in mice deficient in neuronal nitric oxide synthase. Science 265:1883–1885.1994). [PubMed: 7522345]

15. Brenman JE, Chao DS, Gee SH, McGee AW, Craven SE, Santillano DR, Wu Z, Huang F, Xia H, Peters MF, Froehner SC, Bredt DS (Interaction of nitric oxide synthase with the postsynaptic density protein PSD-95 and alpha1-syntrophin mediated by PDZ domains. Cell 84:757–767.1996). S0092–8674(00)81053–3 [pii] [PubMed: 8625413]

16. Christopherson KS, Hillier BJ, Lim WA, Bredt DS (PSD-95 assembles a ternary complex with the N-methyl-D-aspartic acid receptor and a bivalent neuronal NO synthase PDZ domain. J Biol Chem 274:27467–27473.1999). [PubMed: 10488080]

17. Kornau HC, Schenker LT, Kennedy MB, Seeburg PH (Domain interaction between NMDA receptor subunits and the postsynaptic density protein PSD-95. Science 269:1737–1740.1995). [PubMed: 7569905]

18. Aarts M, Liu Y, Liu L, Besshoh S, Arundine M, Gurd JW, Wang YT, Salter MW, Tymianski M (Treatment of ischemic brain damage by perturbing NMDA receptor- PSD-95 protein interactions. Science 298:846–850.2002). 10.1126/science.1072873 [doi];298/5594/846 [pii] [PubMed: 12399596]

19. Sattler R, Xiong Z, Lu WY, Hafner M, MacDonald JF, Tymianski M (Specific coupling of NMDA receptor activation to nitric oxide neurotoxicity by PSD-95 protein. Science 284:1845–1848.1999). [PubMed: 10364559]

20. Zhou L, Li F, Xu HB, Luo CX, Wu HY, Zhu MM, Lu W, Ji X, Zhou QG, Zhu DY (Treatment of cerebral ischemia by disrupting ischemia-induced interaction of nNOS with PSD-95. Nat Med 16:1439–1443.2010). nm.2245 [pii];10.1038/nm.2245 [doi] [PubMed: 21102461]

21. Hu Z, Bian X, Liu X, Zhu Y, Zhang X, Chen S, Wang K, Wang Y (Honokiol protects brain against ischemia-reperfusion injury in rats through disrupting PSD95-nNOS interaction. Brain Res 1491:204–212.2013). S0006-8993(12)01779-9 [pii];10.1016/j.brainres.2012.11.004 [doi] [PubMed: 23148950]

22. Wu S, Yue Y, Tian H, Tao L, Wang Y, Xiang J, Wang S, Ding H (Tramiprosate protects neurons against ischemic stroke by disrupting the interaction between PSD95 and nNOS. Neuropharmacology 83:107–117.2014). S0028-3908(14)00136-1 [pii];10.1016/j.neuropharm.2014.04.010 [doi] [PubMed: 24769446]

23. Mo SF, Liao GY, Yang J, Wang MY, Hu Y, Lian GN, Kong LD, Zhao Y (Protection of neuronal cells from excitotoxicity by disrupting nNOS-PSD95 interaction with a small molecule SCR-4026. Brain Res 1648:250–256.2016). S0006-8993(16)30486-3 [pii];10.1016/j.brainres.2016.07.012 [doi] [PubMed: 27421179]

24. Lin YH, Liang HY, Xu K, Ni HY, Dong J, Xiao H, Chang L, Wu HY, Li F, Zhu DY, Luo CX (Dissociation of nNOS from PSD-95 promotes functional recovery after cerebral ischaemia in mice through reducing excessive tonic GABA release from reactive astrocytes. J Pathol 244:176–188.2018). 10.1002/path.4999 [doi] [PubMed: 29053192]
25. Luo CX, Lin YH, Qian XD, Tang Y, Zhou HH, Jin X, Ni HY, Zhang FY, Qin C, Li F, Zhang Y, Wu HY, Chang L, Zhu DY (Interaction of nNOS with PSD-95 negatively controls regenerative repair after stroke. J Neurosci 34:13535–13548.2014). 34/40/13535 [pii];10.1523/JNEUROSCI.1305-14.2014 [doi] [PubMed: 25274829]
26. Wang DL, Qian XD, Lin YH, Tian BB, Liang HY, Chang L, Wu HY, Zhu DY, Luo CX (ZL006 promotes migration and differentiation of transplanted neural stem cells in male rats after stroke. J Neurosci Res 95:2409–2419.2017). 10.1002/jnr.24068 [doi] [PubMed: 28512996]
27. Tao F, Tao YX, Gonzalez JA, Fang M, Mao P, Johns RA (Knockdown of PSD-95/SAP90 delays the development of neuropathic pain in rats. Neuroreport 12:3251–3255.2001). [PubMed: 11711866]
28. Tao YX, Huang YZ, Mei L, Johns RA (Expression of PSD-95/SAP90 is critical for N-methyl-D-aspartate receptor-mediated thermal hyperalgesia in the spinal cord. Neuroscience 98:201–206.2000). S0306-4522(00)00193-7 [pii] [PubMed: 10854750]
29. Florio SK, Loh C, Huang SM, Iwamaye AE, Kitto KF, Fowler KW, Treiberg JA, Hayflick JS, Walker JM, Fairbanks CA, Lai Y (Disruption of nNOS-PSD95 protein-protein interaction inhibits acute thermal hyperalgesia and chronic mechanical allodynia in rodents. Br J Pharmacol 158:494–506.2009). BPH300 [pii];10.1111/j.1476-5381.2009.00300.x [doi] [PubMed: 19732061]
30. Carey LM, Lee WH, Gutierrez T, Kulkarni PM, Thakur GA, Lai YY, Hohmann AG (Small molecule inhibitors of PSD95-nNOS protein-protein interactions suppress formalin-evoked Fos protein expression and nociceptive behavior in rats. Neuroscience 349:303–317.2017). S0306-4522(17)30146-X [pii];10.1016/j.neuroscience.2017.02.055 [doi] [PubMed: 28285942]
31. Lee WH, Xu Z, Ashpole NM, Hudmon A, Kulkarni PM, Thakur GA, Lai YY, Hohmann AG (Small molecule inhibitors of PSD95-nNOS protein-protein interactions as novel analgesics. Neuropharmacology 97:464–475.2015). S0028-3908(15)00228-2 [pii];10.1016/j.neuropharm.2015.05.038 [doi] [PubMed: 26071110]
32. Chizh BA, Headley PM (NMDA antagonists and neuropathic pain--multiple drug targets and multiple uses. Curr Pharm Des 11:2977–2994.2005). [PubMed: 16178757]
33. Parsons CG (NMDA receptors as targets for drug action in neuropathic pain. Eur J Pharmacol 429:71–78.2001). S0014299901013073 [pii] [PubMed: 11698028]
34. Li Z, Mao Y, Liang L, Wu S, Yuan J, Mo K, Cai W, Mao Q, Cao J, Bekker A, Zhang W, Tao YX (The transcription factor C/EBPbeta in the dorsal root ganglion contributes to peripheral nerve trauma-induced nociceptive hypersensitivity. Sci Signal 102017). 10/487/eaam5345 [pii];10.1126/scisignal.aam5345 [doi]
35. Li Z, Gu X, Sun L, Wu S, Liang L, Cao J, Lutz BM, Bekker A, Zhang W, Tao YX (Dorsal root ganglion myeloid zinc finger protein 1 contributes to neuropathic pain after peripheral nerve trauma. Pain 156:711–721.2015). 10.1097/j.pain.0000000000000103 [doi] [PubMed: 25630025]
36. Xu JT, Zhao JY, Zhao X, Ligons D, Tiwari V, Atianjoh FE, Lee CY, Liang L, Zang W, Njoku D, Raja SN, Yaster M, Tao YX (Opioid receptor-triggered spinal mTORC1 activation contributes to morphine tolerance and hyperalgesia. J Clin Invest 124:592–603.2014). 70236 [pii];10.1172/JCI70236 [doi] [PubMed: 24382350]
37. Zhao X, Tang Z, Zhang H, Atianjoh FE, Zhao JY, Liang L, Wang W, Guan X, Kao SC, Tiwari V, Gao YJ, Hoffman PN, Cui H, Li M, Dong X, Tao YX (A long noncoding RNA contributes to neuropathic pain by silencing Kcna2 in primary afferent neurons. Nat Neurosci 16:1024–1031.2013). nn.3438 [pii];10.1038/nn.3438 [doi] [PubMed: 23792947]
38. Liaw WJ, Stephens RL, Jr., Binns BC, Chu Y, Sepkuty JP, Johns RA, Rothstein JD, Tao YX (Spinal glutamate uptake is critical for maintaining normal sensory transmission in rat spinal cord. Pain 115:60–70.2005). S0304-3959(05)00053-9 [pii];10.1016/j.pain.2005.02.006 [doi] [PubMed: 15836970]
39. Park JS, Voitenko N, Petralia RS, Guan X, Xu JT, Steinberg JP, Takamiya K, Sotnik A, Kopach O, Huganir RL, Tao YX (Persistent inflammation induces GluR2 internalization via NMDA receptor-

triggered PKC activation in dorsal horn neurons. J Neurosci 29:3206–3219.2009). 29/10/3206 [pii];10.1523/JNEUROSCI.4514-08.2009 [doi] [PubMed: 19279258]

40. Tao YX, Rumbaugh G, Wang GD, Petralia RS, Zhao C, Kauer FW, Tao F, Zhuo M, Wenthold RJ, Raja SN, Huganir RL, Bredt DS, Johns RA (Impaired NMDA receptor-mediated postsynaptic function and blunted NMDA receptor-dependent persistent pain in mice lacking postsynaptic density-93 protein. J Neurosci 23:6703–6712.2003). 23/17/6703 [pii] [PubMed: 12890763]
41. Zhao JY, Liang L, Gu X, Li Z, Wu S, Sun L, Atianjoh FE, Feng J, Mo K, Jia S, Lutz BM, Bekker A, Nestler EJ, Tao YX (DNA methyltransferase DNMT3a contributes to neuropathic pain by repressing Kcna2 in primary afferent neurons. Nat Commun 8:147122017). ncomms14712 [pii]; 10.1038/ncomms14712 [doi] [PubMed: 28270689]
42. Attal N, Brasseur L, Parker F, Chauvin M, Bouhassira D (Effects of gabapentin on the different components of peripheral and central neuropathic pain syndromes: a pilot study. Eur Neurol 40:191–200.1998). 10.1159/000007979 [PubMed: 9813401]
43. Akyuz G, Kuru P (Systematic Review of Central Post Stroke Pain: What Is Happening in the Central Nervous System? Am J Phys Med Rehabil 95:618–627.2016). 10.1097/PHM. 0000000000000542 [doi] [PubMed: 27175563]
44. Kumar A, Bhoi SK, Kalita J, Misra UK (Central Poststroke Pain Can Occur With Normal Sensation. Clin J Pain 32:955–960.2016). 10.1097/AJP.0000000000000344 [doi]; 00002508-201611000-00006 [pii] [PubMed: 27749332]
45. Vartiainen N, Perchet C, Magnin M, Creac'h C, Convers P, Nighoghossian N, Mauguiere F, Peyron R, Garcia-Larrea L (Thalamic pain: anatomical and physiological indices of prediction. Brain 139:708–722.2016). awv389 [pii];10.1093/brain/awv389 [doi] [PubMed: 26912644]
46. Blasi F, Herisson F, Wang S, Mao J, Ayata C (Late-onset thermal hypersensitivity after focal ischemic thalamic infarcts as a model for central post-stroke pain in rats. J Cereb Blood Flow Metab 35:1100–1103.2015). jcbfm201573 [pii];10.1038/jcbfm.2015.73 [doi] [PubMed: 25899295]
47. Hanada T, Kurihara T, Tokudome M, Tokimura H, Arita K, Miyata A (Development and pharmacological verification of a new mouse model of central post-stroke pain. Neurosci Res 78:72–80.2014). S0168-0102(13)00202-2 [pii];10.1016/j.neures.2013.09.005 [doi] [PubMed: 24055601]
48. Yang F, Fu H, Lu YF, Wang XL, Yang Y, Yang F, Yu YQ, Sun W, Wang JS, Costigan M, Chen J (Post-stroke pain hypersensitivity induced by experimental thalamic hemorrhage in rats is region-specific and demonstrates limited efficacy of gabapentin. Neurosci Bull 30:887–902.2014). 10.1007/s12264-014-1477-5 [doi];10.1007/s12264-014-1477-510.1007/s12264-014-1477-5 [doi]; 10.1007/s12264-014-1477-5 [pii] [PubMed: 25370442]
49. Takami K, Fujita-Hamabe W, Harada S, Tokuyama S (Abeta and Adelta but not C-fibres are involved in stroke related pain and allodynia: an experimental study in mice. J Pharm Pharmacol 63:452–456.2011). 10.1111/j.2042-7158.2010.01231.x [doi] [PubMed: 21749395]
50. Castel A, Helie P, Beaudry F, Vachon P (Bilateral central pain sensitization in rats following a unilateral thalamic lesion may be treated with high doses of ketamine. BMC Vet Res 9:592013). 1746-6148-9-59 [pii];10.1186/1746-6148-9-59 [doi] [PubMed: 23537119]
51. Tamiya S, Yoshida Y, Harada S, Nakamoto K, Tokuyama S (Establishment of a central post-stroke pain model using global cerebral ischaemic mice. J Pharm Pharmacol 65:615–620.2013). 10.1111/ jphp.12007 [doi] [PubMed: 23488791]

Author Manuscript

Author Manuscript

Author Manuscript

Highlights

- The thalamus hemorrhagic mice exhibit hyperalgesia phenomena.
- Pre-treatment of ZL006 attenuates hemorrhage-induced thalamic pain.
- ZL006 takes effect by disrupting the PSD-95-nNOS protein-protein interaction in thalamic neurons

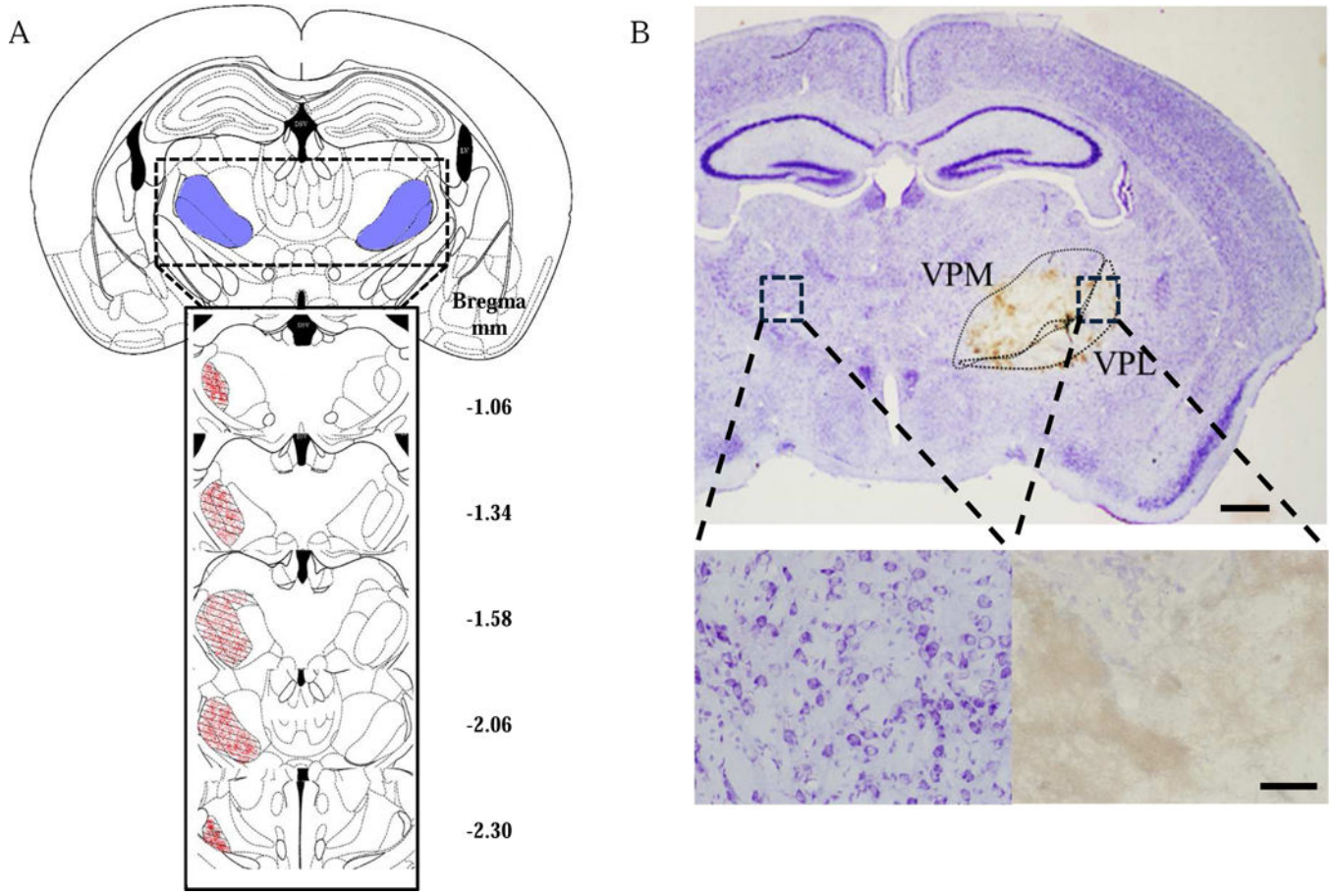

Fig. 1.

Thalamic hemorrhage in the adult mouse. (A) Schematic illustration of the spatial extent of the hemorrhagic lesion induced by the microinjection of collagenase IV (0.01 U, 10 nl) into the ventral posterior medial nuclei (VPM) and ventral posterior lateral nuclei (VPL) of the thalamus. The areas filled with red spots represent lesion sites. (B) Top: Representative photograph of a coronal brain section stained with Cresyl Violet from a mouse 3 days after collagenase type IV microinjection. The area of the injected site is indicated by a dotted line. Scale bar: 500 μm. Bottom: High magnifications of t he dashed squares in the top photograph on the ipsilateral and contralateral sides. Scale bar: 100 μm.

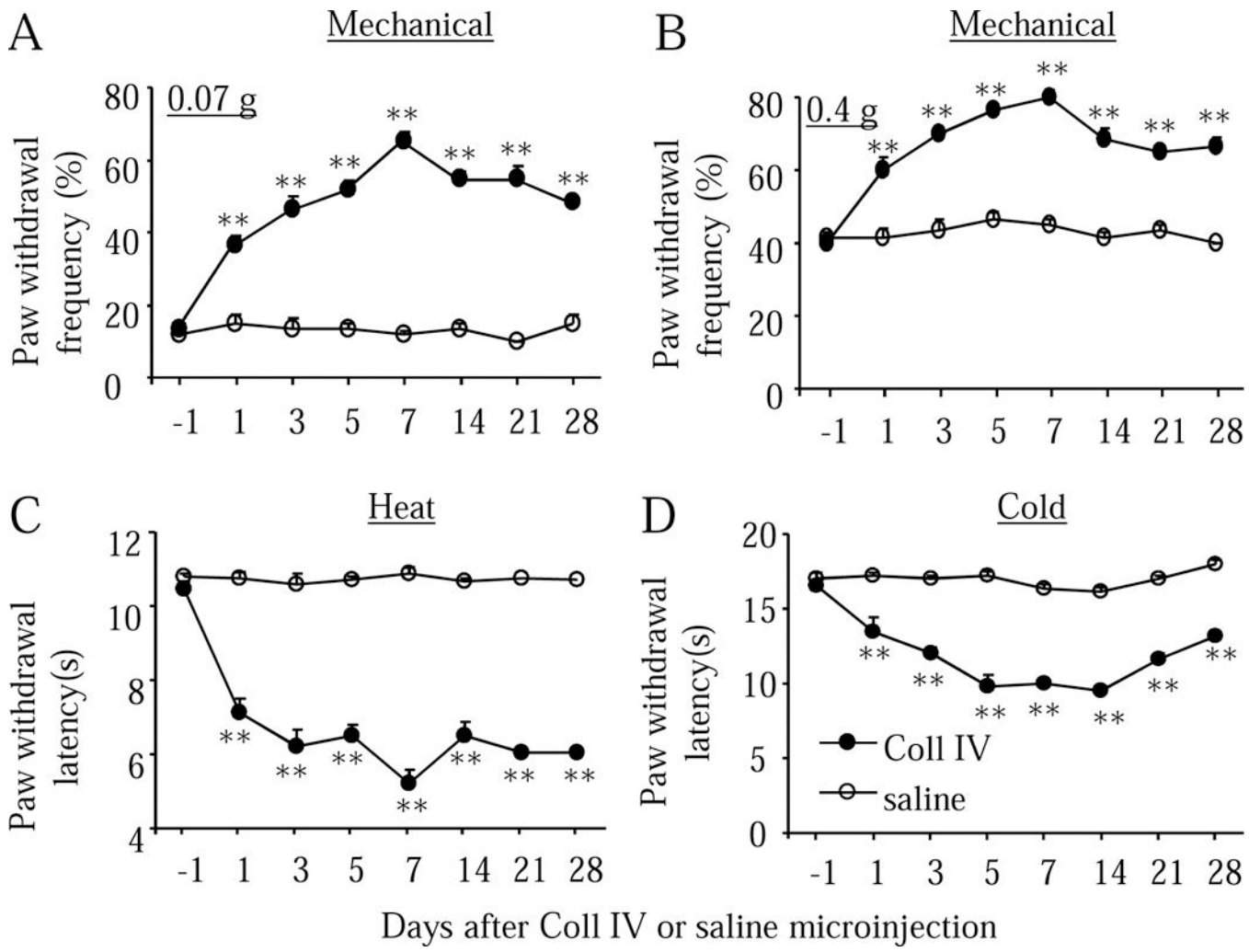

Fig. 2.

Thalamic hemorrhage produces early onset and long-lasting pain hypersensitivities on the contralateral side. The microinjection of collagenase IV (Coll IV), but not saline, into the ventral posterior medial nuclei and ventral posterior lateral nuclei led to the increases in paw withdrawal frequencies in responses to 0.07 g (A) and 0.4 g (B) von Frey filaments and the decreases in paw withdrawal latencies to heat (C) and cold (D) stimuli on the contralateral side. n = 10 mice per group. $^{**}P < 0.01$ *vs* the saline-treated group at the corresponding time points.

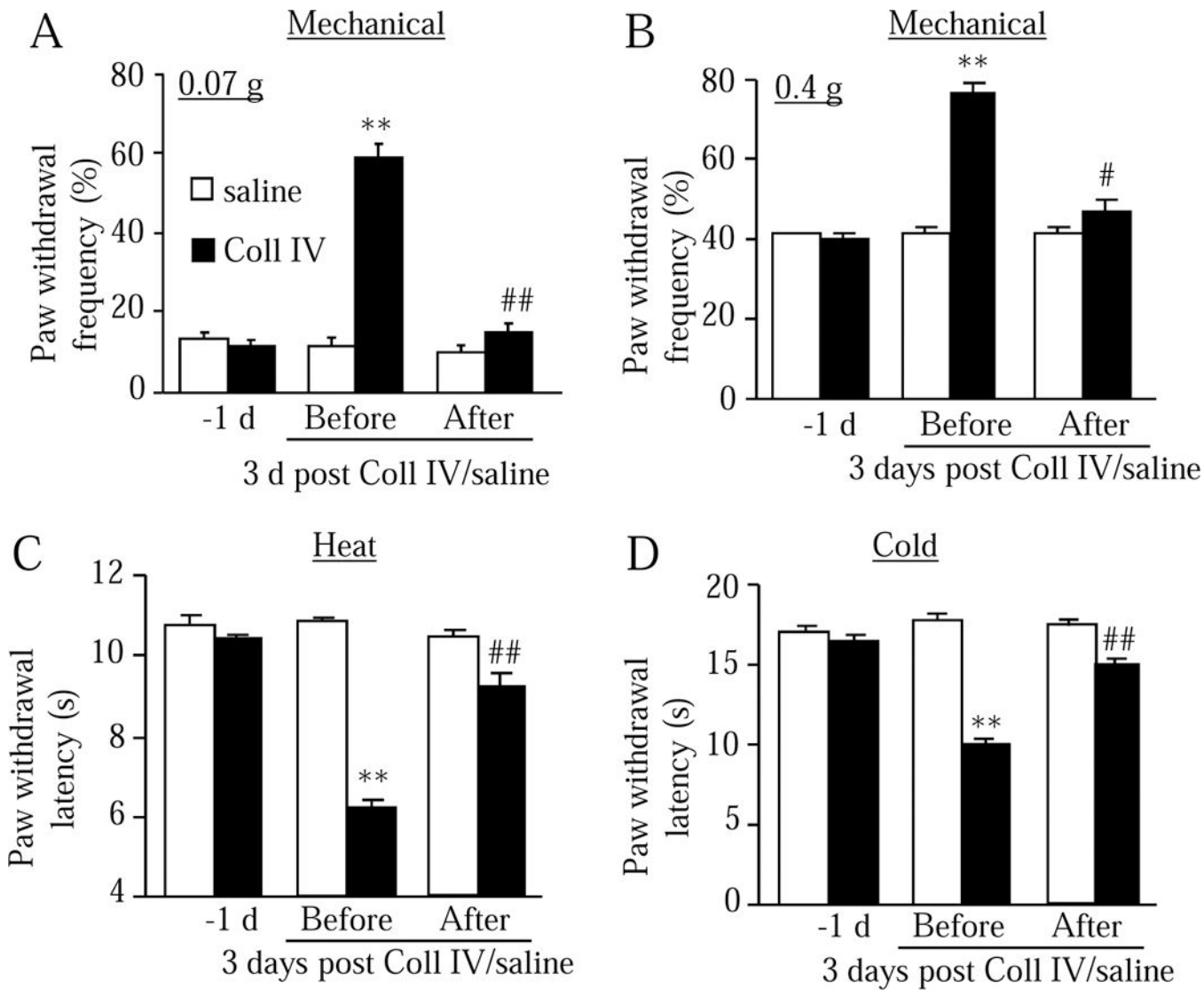

Fig. 3.

Effect of intraperitoneal (i.p.) administration of gabapentin on the hemorrhage-induced thalamic pain in mice. Behavior tests were carried out one day before Coll IV or saline microinjection and before and 30 min after i.p. administration of gabapentin on day 3 after Coll IV or saline microinjection. Gabapentin (20 mg/kg) significantly blocked the Coll IV-induced increases in paw withdrawal frequencies to 0.07 g (A) and 0.4 g (B) von Frey filaments and decreases in paw withdrawal latencies to heat (C) and cold (D) stimuli on the contralateral side on day 3 after Coll IV microinjection. Gabapentin at the dose used did not alter basal responses on day 3 after saline microinjection. n = 10 mice per group. $^{**}P < 0.01$ *vs* the corresponding baseline before Coll IV microinjection. $^{\#}P < 0.05$ or $^{\#\#}P < 0.01$ *vs* the corresponding treated group before gabapentin administration.

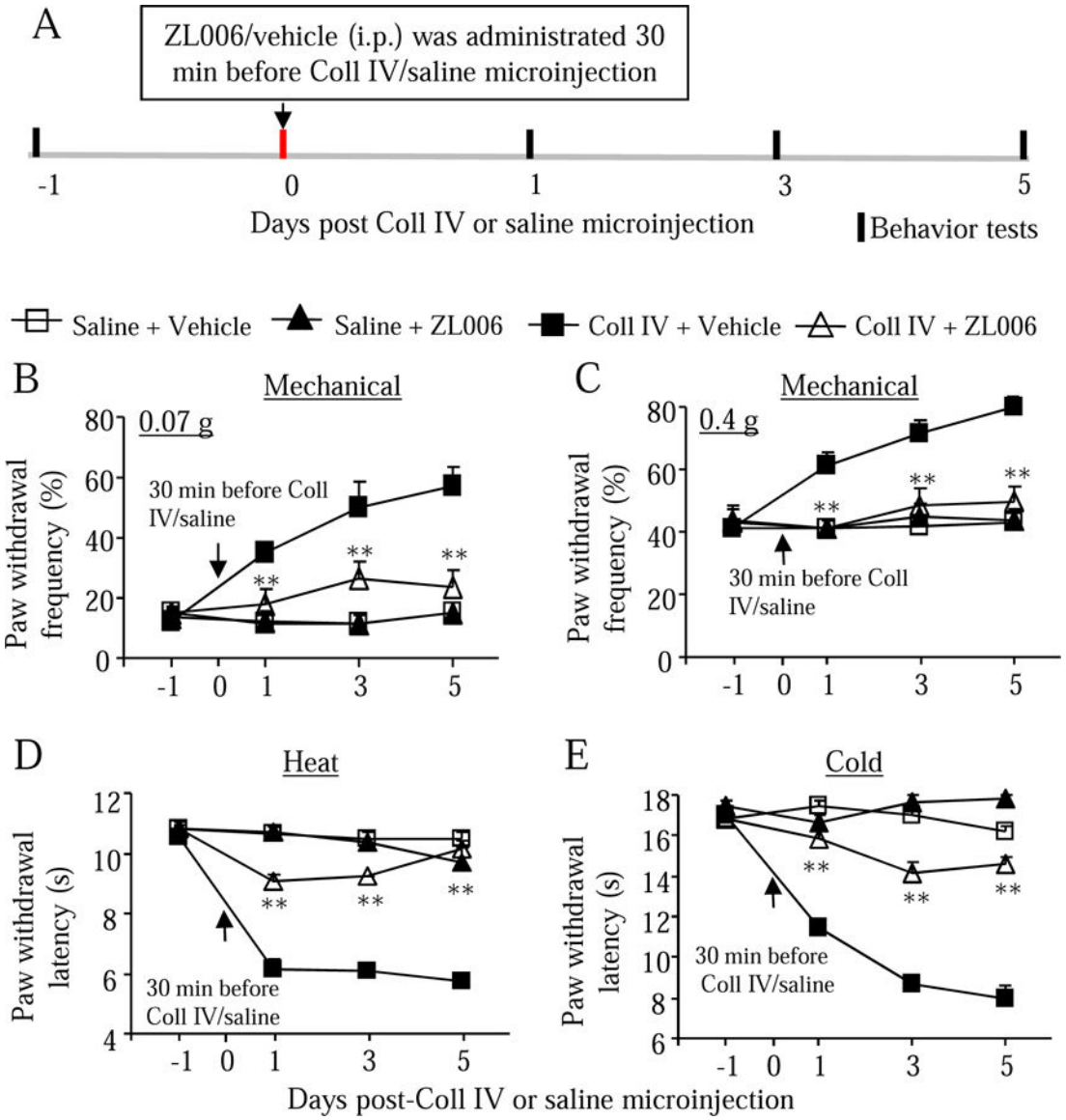

Fig. 4.

Effect of systemic pre-administration of ZL006 on the hemorrhage-induced thalamic pain on the contralateral side. ZL006 (10 mg/kg, i.p.) or vehicle was given 30 min before Coll IV or saline microinjection (A). Behavioral tests were carried out one day before Coll IV or saline microinjection and on days 1, 3, and 5 after Coll IV or saline microinjection (A). ZL006, but not vehicle, significantly attenuated the Coll IV-induced increases in paw withdrawal frequencies to 0.07 g (B) and 0.4 G (C) von Frey filaments and reductions in paw withdrawal latencies to heat and cold (E) on days 1, 3 and 5 after Coll IV microinjection on the contralateral side. ZL006 did not alter basal paw withdrawal frequencies and latencies on the contralateral side from the saline-microinjected group (B-E). n = 10 mice per group. $^{**}P < 0.01$ *vs* the Coll IV plus vehicle group at the corresponding days.

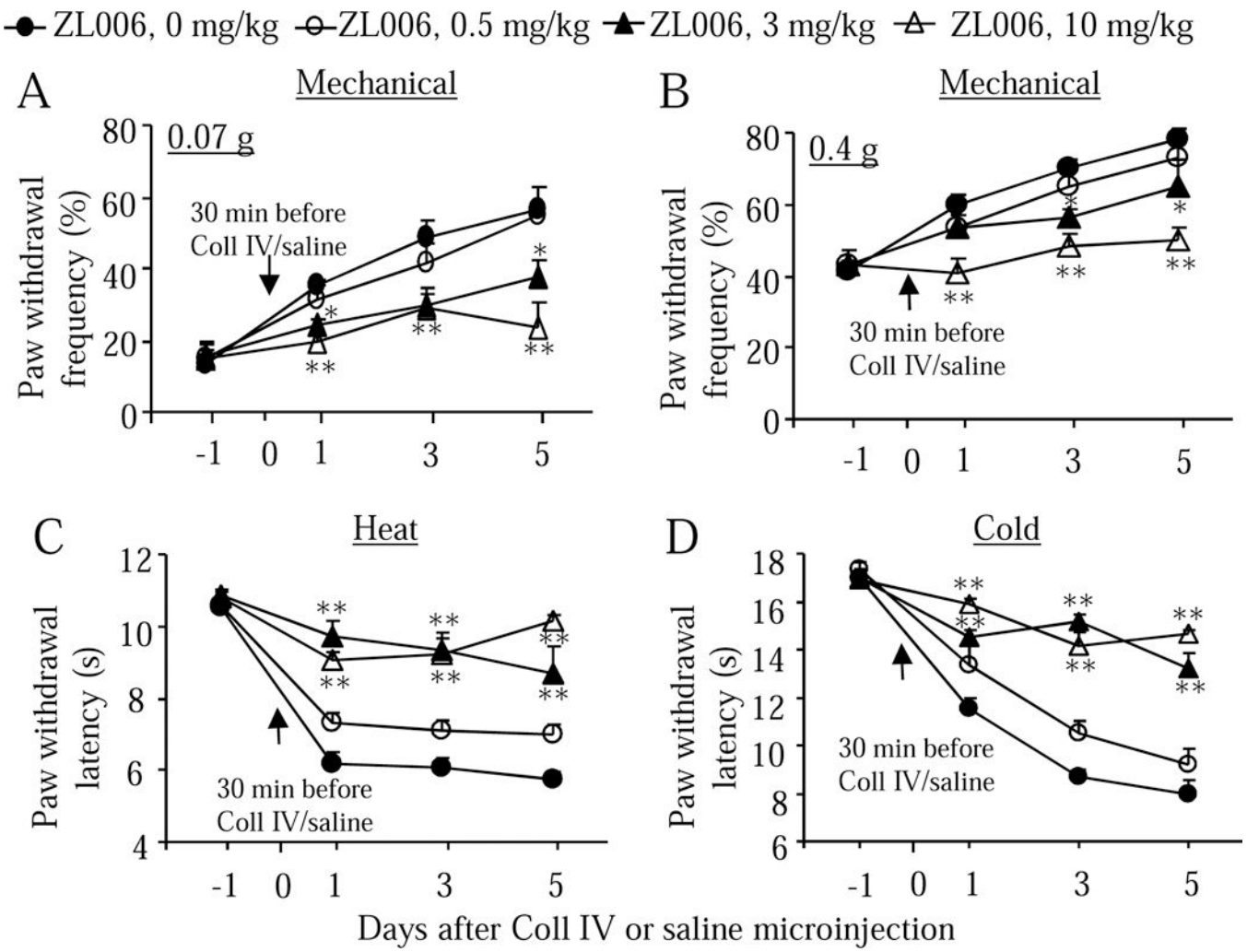

Fig. 5.

Dose-dependent effects of pre-administration of ZL006 on the hemorrhage-induced thalamic pain on the contralateral side. Three doses of ZL006 (0.5, 3, 10 mg/kg; i.p.) or vehicle (ZL006 at 0 mg/kg) were given 30 min before Coll IV or saline microinjection. Behavioral tests were carried out one day before Coll IV or saline microinjection and on days 1, 3, and 5 after Coll IV or saline microinjection. Paw withdrawal frequencies in response to 0.07 g (A) and 0.4 g (B) von Frey filaments and paw withdrawal latency to heat (C) and cold (D) stimuli on the contralateral side. n = 10 mice per group. $*P < 0.05$ or $**P < 0.01$ *vs* the Coll IV plus vehicle group at the corresponding days.

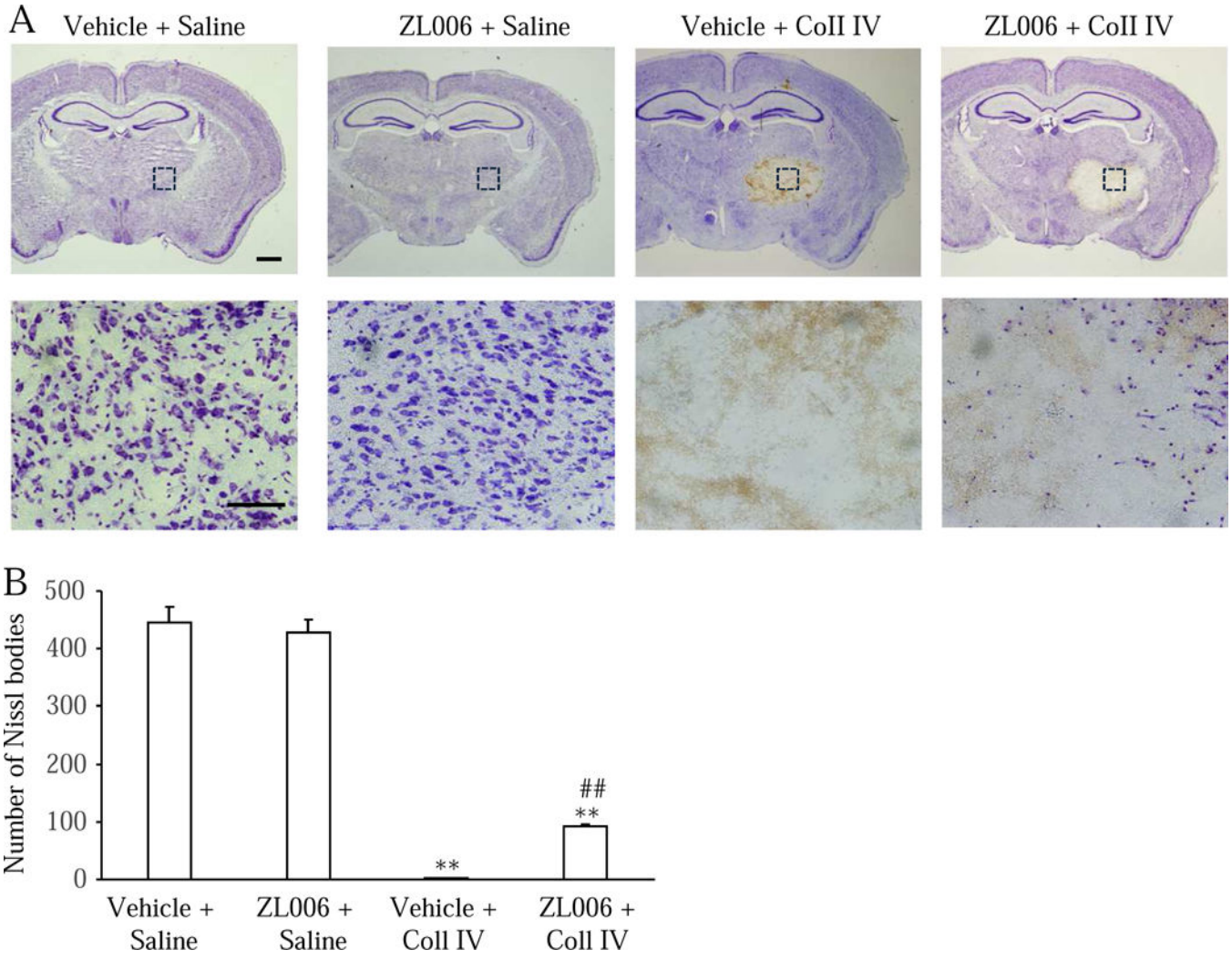

Fig. 6.

Effect of systemic pre-administration of ZL006 on the hemorrhage-induced thalamic lesion. (A) Representative photographs of coronal brain sections stained with Nissl from the treated groups as indicated on day 5 after Coll IV or saline microinjection. Top: photographs of whole brain sections, scale bar: 500 μm. Bottom: hi gh magnification of the dashed squares in the corresponding top photographs, Scale bar: 100 μm. (B) Numbers of Nissl-stained cells in the ventral posterior medial nuclei and ventral posterior lateral nuclei of the thalamus of the different treated groups as indicated. n = 6 mice per group. $^{**}P < 0.01$ *vs* the vehicle plus saline-treated group. $^{\#\#}P < 0.01$ *vs* the vehicle plus Coll IV-treated group.

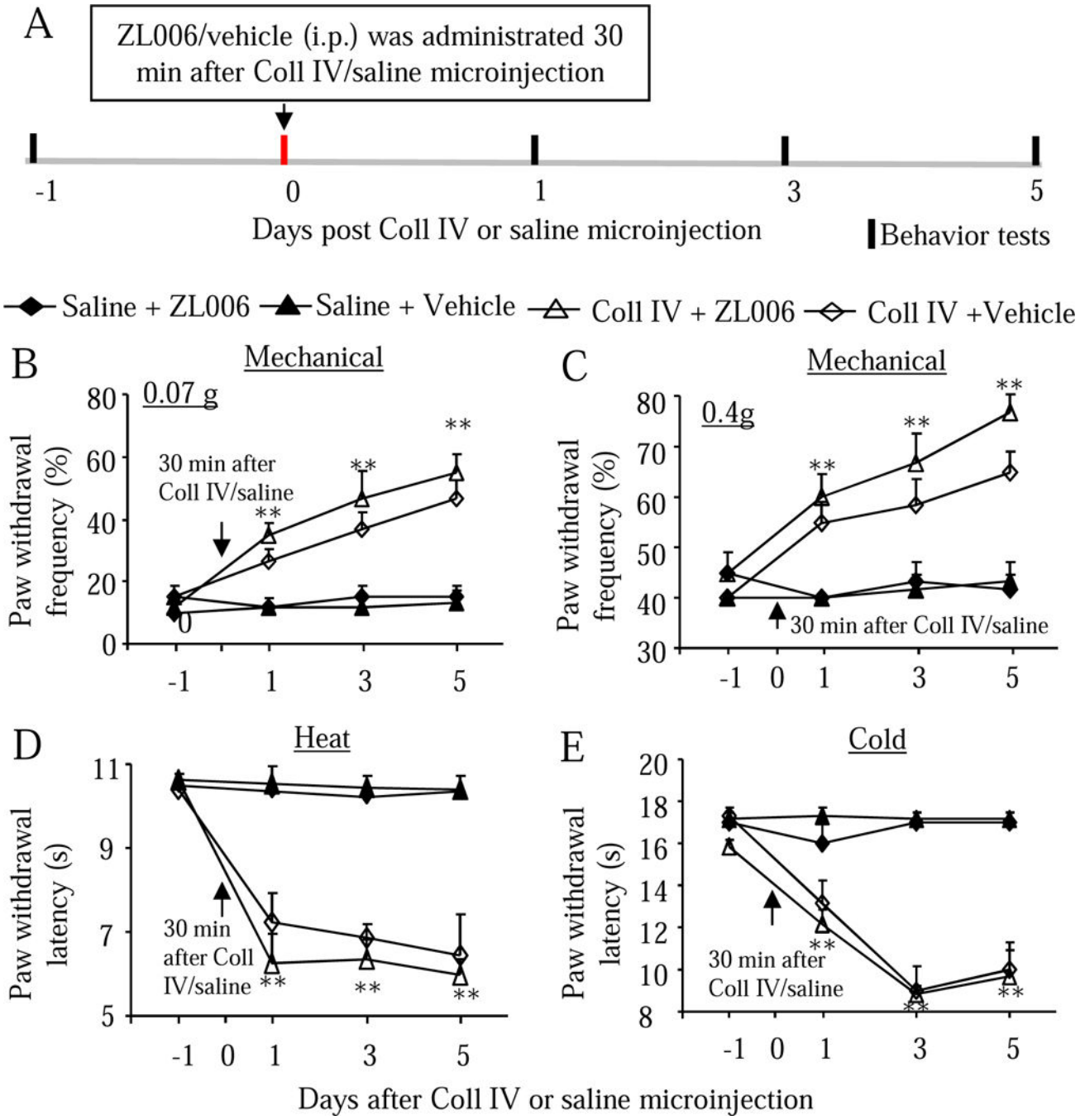

Fig. 7.

Effect of systemic post-administration of ZL006 on the hemorrhage-induced thalamic pain on the contralateral side. ZL006 (10 mg/kg, i.p.) or vehicle was given 30 min after Coll IV or saline microinjection (A). Behavioral tests were carried out one day before Coll IV or saline microinjection and on days 1, 3, and 5 after Coll IV or saline microinjection (A). ZL006 did not affect the Coll IV-induced increases in paw withdrawal frequencies to 0.07 g (B) and 0.4 G (C) von Frey filaments and reductions in paw withdrawal latencies to heat (D) and cold (E) on days 1, 3 and 5 after Coll IV microinjection on the contralateral side. ZL006

also did not alter basal paw withdrawal frequencies and latencies on the contralateral side from the saline-microinjected group (B-E). n = 10 mice per group. $^{**}P < 0.01$ *vs* the corresponding baseline (one day before Coll IV or saline microinjection).

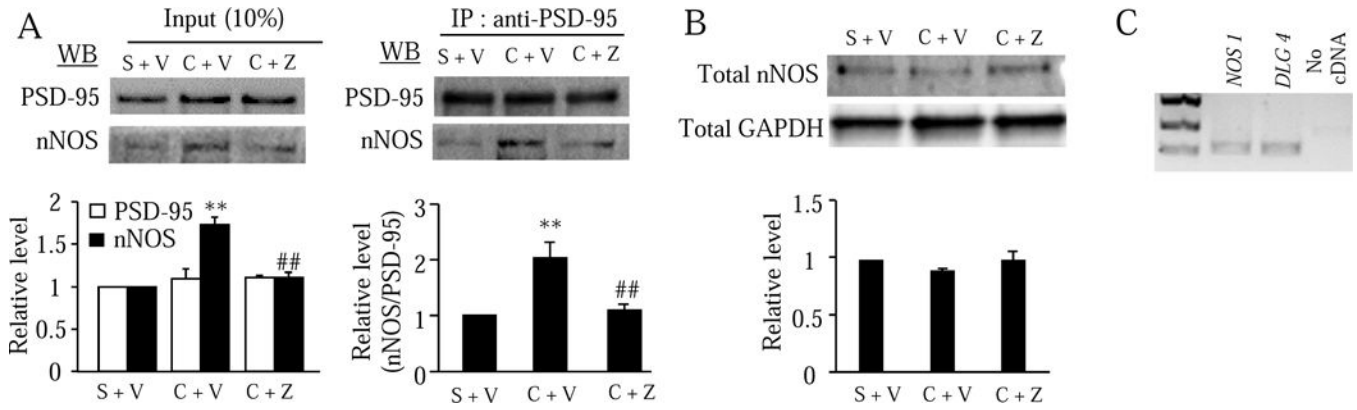

Fig. 8.

Effect of systemic pre-administration of ZL006 on the hemorrhage-induced increase in PSD-95-nNOS protein-protein interaction in the ipsilateral thalamus 3 days after Coll IV or saline microinjection. S: saline. V: vehicle. C: Coll IV. Z: ZL006. (A) Left: Input indicating the relative level of PSD-95 and nNOS in the crude membrane fraction (input) from the ipsilateral thalamus of the different treated groups. The band densities for the saline plus vehicle-treated groups were set as 100%. The relative densities from the remaining groups were determined by dividing by the optical densities from these groups by the values of the corresponding saline plus vehicle-treated groups. Right: Co-immunoprecipitation (IP) of nNOS and PSD-95 with anti-PSD-95 serum in the crude membrane fraction from the ipsilateral thalamus of the different treated groups indicated. The relative level of nNOS in the saline plus vehicle-treated group was set as 100%. The relative levels of nNOS from the remaining groups were determined by dividing the optical density values from these groups by the value of the saline plus vehicle-treated group after each was normalized to its corresponding PSD-95 density. n = 3 biological repeats (6 mice) per group. $^{**}P < 0.01$ *vs* the corresponding saline plus vehicle-treated group. $^{\#\#}P < 0.01$ *vs* the corresponding Coll IV plus vehicle-treated group. (B) The total level of nNOS in the cytosolic and membrane fractions from the ipsilateral thalamus of the different treated groups indicated. n = 3 biological repeats (3 mice) per group. GAPDH was used as a loading control. (C) Co-expression of *Nos1* mRNA with *Dlg4* mRNA in the individual neurons from mouse thalamus. n = 3 biological repeats (3 mice).